Author/s:
Garcia-Rosas, R;Portella-Delgado, JM;Tan, Y;NESIC, D

Title:
Nonlinear Observer Based Control Design for an Under-actuated Compliant Robotic Hand

Date:
2016

Citation:
Garcia-Rosas, R., Portella-Delgado, J. M., Tan, Y. & NESIC, D. (2016). Nonlinear Observer Based Control Design for an Under-actuated Compliant Robotic Hand. 2016 Australian Control Conference Aucc 2016, Engineers Australia. https://doi.org/10.1109/AUCC.2016.7867926.

Persistent Link:
https://hdl.handle.net/11343/297900

Nonlinear Observer Based Control Design for an Under-actuated Compliant Robotic Hand

Ricardo Garcia-Rosas, Jhon M. Portella-Delgado, Ying Tan, Dragan Nešić

***Abstract*— This project aims at designing control algorithms for an under-actuated compliant adaptive prosthetic hand to perform a complex task of grasping and manipulating of an unknown object. As multiple objectives are considered, if one controller is designed for one control objective, a hybrid controller is needed to coordinate different controllers to perform complex tasks. This project thus tries to apply recently developed framework of systems of funnels to the under-actuated compliant adaptive prosthetic hand to design this hybrid controller. In order to apply System of Funnels, each controller has to have the flexibility to obtain any given domain of attraction by tuning its parameters. This paper proposed nonlinear observer based nonlinear PID controllers for Grasp Approach and Grasp Stabilization. The nonlinear observer estimates the needed velocity of the under-actuated compliant adaptive prosthetic hand, which is needed for nonlinear PID controller. By tuning parameters of PID controller and nonlinear observers appropriately, any desired domain of attraction for each control objective can be achieved. Our next step is to design some manipulation controller with adjustable domain of attraction in order to apply the framework of System of Funnels.**

I. Introduction

As technologies develop, highly biomimetic anthropomorphic hands such as the one developed by Xu and Todorov [1] have been developed. These robotic hands are extraordinarily close to human hands in design and performance, leading to a huge potential in the prosthetics field. Usually prosthetic devices are constrained in their size, weight and control capabilities because of the need of comfort and functionality requirement from the user, who usually has limited control capabilities due to the limitations of current human-brain interfaces. Therefore, most anthropomorphic and advanced hand prosthesis have under-actuated mechanisms that trade-off functionality and dexterity for the compactness and weight limits that prosthetic devices pose.

One of the challenges in robotic manipulators is to design a suitable control mechanism to achieve different desired control objectives. This same challenge applies to modern robotic hand prosthesis. For a single control objective such as performing tracking with a prosthetic hand, it is not too difficult to design a low level controller (for example, a simple PD controller [2] or PID controller) to ensure that the actuators behave in the desired manner. Another example for the single control objective is to control the force to which the manipulator is applying in order to interact with an unknown object by using a tension controller, see for example, Lee et. al. [3]. For prosthetic devices, it is desired to achieve multiple control objectives. For example, an under-actuated hand needs to grasp and manipulate of an unknown object. Under such a situation, a single position controller or a single force controller is not sufficient to perform the complex task.

Different hybrid controllers have been proposed to achieve multiple objectives simultaneously. These hybrid controllers usually have different control laws for different control objectives and the switching can happen when changing from one control objective to another. Luo proposed a sliding mode based impedance controller that could achieve the task by restricting the force while performing position tracking without considering the interaction between the unknown object and the prosthetic device [4]. Kubo and Ohnishi proposed a hybrid controller that fuses together passivity based position and force controllers to achieve object stabilization through multiple fingers without providing any theoretic proof, though experimental results were convincing [5]. A more rigorous stability proof of a switching between a position controller and a force controller for a manipulator was provided by Heck et. al. where the stability analysis was performed within given switching surfaces [6]. Recently, the concept of funnels has gained a lot of attention in stability and performance analysis of robotic systems, see for example [7], [8] and reference therein. Generally, the concept of funnels provides a measure of a dynamic system's behavior along the trajectories and thus can be used to measure the robustness of the controller. An optimization technique by using sums of squares (SOS) programming to maximize the size of such funnels has been proposed [7]. The effectiveness of funnel-based design framework has been shown in [8]. It was shown that this framework not only provides robust off-line trajectory computation and controller design, but can also be used to provide robust on-line trajectory planning for a given controller.

A significant recent contribution by Shvartsman is a framework for designing hybrid controllers through System of Funnels [9]. This framework provides a set of tools to assist the design of hybrid controller to achieve the desired performance for each control objective as well as the overall task, and proof of its stability; making it appealing in the hybrid controller design for the under-actuated compliant adaptive prosthetic hand to perform the complex tasks. In order to apply the framework of System of Funnels, the first step is to design a controller for each control objective with a flexibility to tune its domain of attraction. In this project, the complex task of grasping and manipulating an unknown object is considered. In particular, this paper focuses on the preliminary work to develop a System of Funnels, which is the development of the Grasp Approach and Grasp Stabilization control objectives and their stability

This research was supported by the Australia Research Council under the Future Fellowship Scheme FT0991385

Ricardo Garcia-Rosas is sponsored by CONACYT Mexico

Ricardo Garcia-Rosas, Jhon M. Portella-Delgado, Ying Tan, Dragan Nešić The University of Melbourne, VIC 3010, Australia. yingt@unimelb.edu.au; dnesic@unimelb.edu.au

analysis. As the velocity of the under-actuated compliant adaptive prosthetic hand is usually not measurable, instead of using numerical method to estimate the velocity, this paper proposed nonlinear observer based nonlinear PID controllers for Grasp Approach and Grasp Stabilization respectively. By applying standard Lyapunov direct method and Krasovskii-LaSalle's invariance principle, the main result (Theorem 1) shows that the domain of attraction of the closed-loop system (both for Grasp Approach and Grasp Stabilization) can be made arbitrarily large by tuning the observer gains and PID controller gains properly; demonstrating their stability independently. The obtained result makes it possible to apply the framework of System of Funnels to the under-actuated compliant adaptive prosthetic hand to preform complex tasks such as grasping and manipulating.

The set of real numbers is denoted as $\mathbb{R}$. For a square matrix $A \in R^{n\times n}$, $\lambda_{max}(A)$ and $\lambda_{min}(A)$ are its largest and smallest eigenvalues of A respectively. A continuous function $\beta : R_{\geq 0} \times R_{\geq 0} \rightarrow R_{\geq 0}$ is of class $\mathcal{KL}$ if it is nondecreasing in its first argument and converging to zero in its second argument

II. Modeling of an Under-actuated finger

A. System description

The model used is based on the SDM and iHY hands [10]. These hands are composed of under-actuated compliant adaptive fingers. The system is described by a tendon-pulley representation with flexible joints [11]. As can be seen in Figure 1, it consists of two links. One is the proximal link (length l_p and mass m_p) and the other is the distal link (length l_d and mass m_d). These links are attached by flexible joints and actuated through a tendon. The proximal joint attaches the proximal link to the plam and has stiffness k_p. The distal joint attaches the distal link to the proximal link and has stiffness k_d. The equvilant pulleys have radius r_p and r_d respectively. Where q_p is the proximal phalanx's joint displacement and q_d the distal phalanx's joint displacement in radians. q_{p0} and q_{d0} represent the joint's spring rest position.

The tendon actuating the finger is controlled by a single motor and pulley with radius r_a. For the simplicity of analysis, it is assumed that $r_a = r_p$. The motor displacement is represented by q_a. The motor can actuate the finger by setting the cable tension F_a. All contact forces interacting with the finger can be transformed and represented in forces perpendicular to the finger. F_c represents the contact forces given by the interaction between an object and the finger. Since the task involved deals with precision grasping and manipulation, only contact forces at the fingertip are considered. Furthermore, disturbance forces F_e can act anywhere on the finger, with F_{ep} representing the disturbance force acting on the proximal link and F_{ed} the disturbance force acting on the distal link. It is important to note that only forces that push on the finger are considered, since these are the forces that could act on the physical system.

The physical meanings of parameters in Figure 1 are summarized in Table I. The finger's motion is thus represented by the generalized coordinates $\mathbf{q} = \begin{bmatrix} q_p & q_d \end{bmatrix}^T$.

Finger Kinematics: The relationship between the actuator pulley and the joint pulleys, or coupling mechanism kinematics, can be written as [12].

$$\dot{q}_a = r_p\dot{q}_p + r_d\dot{q}_d, \tag{1}$$

which can be also represented through the actuator Jacobian J_a, where $J_a = [r_p \quad r_d]$, leading to $\dot{q}_a = J_a\dot{\mathbf{q}}$.

Finger Kinetostatic Analysis: The forces acting on the finger are mapped to general coordinate torques by means of Jacobians [13]. These Jacobians can be obtained through the kinematic analysis [13]. Given the forces acting, they can be decomposed by forces acting along the finger and forces perpendicularly on the finger:

$$\mathbf{F}_c = \begin{bmatrix} F_{cp} & F_{cd} \end{bmatrix}^T, \mathbf{F}_e = \begin{bmatrix} F_{ep} & F_{ed} \end{bmatrix}^T.$$

Through a contact Jacobian J_c and a disturbance force Jacobian J_e it is possible to map these forces to joint torques τ_c and τ_e, representing contact torques and disturbance torques [12]. This representation will be useful for the dynamic analysis of the finger. The contact Jacobian and disturbance Jacobian are given by:

$$J_c = \begin{bmatrix} a_p & 0 \\ a_d + l_p cos(q_d) & a_d \end{bmatrix} J_e = \begin{bmatrix} b_p & 0 \\ b_d + l_p cos(q_d) & b_d \end{bmatrix} \tag{2}$$

where a and b are the distances along the link where the forces are acting. In the case of the contact force, since only precision grasping is being analyzed, $a_d = l_d$. In order to maintain the invertibility of the contact Jacobian, a_p was chosen as half the link's length, i.e. $a_p = l_p/2$. And a

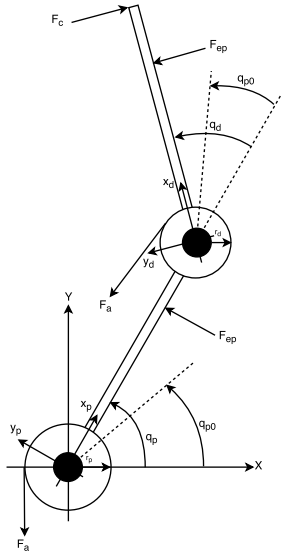

Fig. 1. Under-actuated finger model diagram.

Property	Description
$l_{p/d}$	Proximal/Distal link length (m)
$r_{p/d}$	Proximal/Distal pulley radius (m)
$m_{p/d}$	Proximal/Distal link mass (kg)
$k_{p/d}$	Proximal/Distal joint stiffness (N-m/rad)
$q_{p/d}$	Proximal/Distal joint displacement (rad)
$q_{p/d0}$	Proximal/Distal joint rest position (rad)

TABLE I
Under-actuated finger physical properties.

proximal contact force equal to zero was chosen to satisfy the precision grasp condition $F_{cp} = 0$. The disturbance locations were chosen as $b_p = l_p$ and $b_d = l_d$. Therefore the contact torque $\boldsymbol{\tau}_c$ and disturbance torque $\boldsymbol{\tau}_e$ are:

$$\boldsymbol{\tau}_c = J_c^T \mathbf{F}_c, \qquad \boldsymbol{\tau}_e = J_e^T \mathbf{F}_e. \tag{3}$$

Furthermore, the actuation torque can be described by:

$$\boldsymbol{\tau}_a = J_a^T \mathbf{F}_a, \tag{4}$$

where $\mathbf{F}_a$ is the tendon tension. These torques represent the external forces acting on the finger, and will be used in the development of the dynamic model.

B. Finger Dynamics

Given the finger model, it follows that a common dynamic analysis of a two-link robot is used. The Euler-Lagrange method is standard when modelling the dynamics involved in mechanical systems. Murray's analysis [14] allows a two-link robot to be intuitively represented by the general equation of motion of a mechanical dynamic system.

$$\mathcal{M}(\mathbf{q})\ddot{\mathbf{q}} + \mathcal{C}(\mathbf{q}, \dot{\mathbf{q}})\dot{\mathbf{q}} + g(\mathbf{q}) = \boldsymbol{\tau}. \tag{5}$$

The following assumptions are used to simplify the model [13], [15], [14]

Assumption 1: The effects of gravity are negligible on the finger given the springs acting on the joints.

Assumption 2: There is no friction acting in the joints given their design and construction. However, a Rayleigh dissipation force was included to represent the joint's material inherited dissipative properties.

Assumption 3: The phalanges are rigid links and are assumed to be rods of mass m and length l.

With the help of these assumptions, a dynamic model for an under-actuated finger was obtained through the Euler-Lagrange method [15]. The external forces acting on the finger ($\mathbf{Q}$) are given by the kinetostatic analysis discussed before, and the Rayleigh dissipation force discussed in Assumption 2. The Rayleigh dissipation force takes the form $-\frac{\partial \mathcal{R}}{\partial \dot{\mathbf{q}}}(\dot{\mathbf{q}})$, assuming that the Rayleigh dissipation function $\mathcal{R}(\dot{\mathbf{q}})$ is quadratic [15]. Therefore the external forces are given by:

$$\mathbf{Q} = -\frac{\partial \mathcal{R}}{\partial \dot{\mathbf{q}}}(\dot{\mathbf{q}}) + \boldsymbol{\tau}_c + \boldsymbol{\tau}_e + \boldsymbol{\tau}_a \tag{6}$$

This leads to the following model:

$$\mathcal{M}(\mathbf{q})\ddot{\mathbf{q}} + \mathcal{C}(\mathbf{q}, \dot{\mathbf{q}})\dot{\mathbf{q}} + \mathcal{D}\dot{\mathbf{q}} + \mathcal{K}(\mathbf{q} - \mathbf{q}_0) = \boldsymbol{\tau}_c + \boldsymbol{\tau}_e + \boldsymbol{\tau}_a, \tag{7}$$

where $\mathbf{q}_0$ is the joint rest position. The joint stiffness matrix $\mathcal{K}$ is $\mathcal{K} = \begin{bmatrix} k_p & 0 \\ 0 & k_d \end{bmatrix}$. The diagonal matrix $\mathcal{D}$ is the dissipation matrix satisfying $\mathcal{D} = \mathcal{D}^T \geq 0$. The finger inertia matrix $\mathcal{M}(q)$ is $\begin{bmatrix} \alpha + 2\gamma\cos(q_d) & \eta + 2\gamma\cos(q_d) \\ \eta + 2\gamma\cos(q_d) & \eta \end{bmatrix}$ and $\mathcal{C}(q, \dot{q})$ is the finger Coriolis and centrifugal forces matrix as $\begin{bmatrix} -\gamma\sin(q_d)\dot{q}_d & -\gamma\sin(q_d)(\dot{q}_p + \dot{q}_d) \\ \gamma\sin(q_d)\dot{q}_p & 0 \end{bmatrix}$. The parameters α, γ and η can be computed as [14]:

$$\alpha = \mathcal{I}_{zp} + \mathcal{I}_{zd} + m_p r_p^2 + m_d(l_p^2 + l_p^d)$$
$$\gamma = m_d l_p r_d, \qquad \eta = \mathcal{I}_{zd} + m_d r_d^2,$$

where I_{zp} and I_{zd} are inertia moment in the z-axis of the link p and the link d respectively.

The system (7) can be represented in a state-space with the state $\mathbf{x} = \begin{bmatrix} \mathbf{q} & \dot{\mathbf{q}} \end{bmatrix}^T$, the output $\mathbf{y} = \mathbf{q}$, the control input is $\boldsymbol{\tau}_a$ and the disturbance $\mathbf{w} = \begin{bmatrix} \boldsymbol{\tau}_c^T & \boldsymbol{\tau}_e^T \end{bmatrix}^T$. The disturbances $\boldsymbol{\tau}_c$ appear due to the contact to the object (which can be measured and triggers the controller switching) while the disturbances τ_e are unknown. They represent the performance of the hand being affected by a external force that is not related to the objective (such as the hand hitting the table where the object is). Usually, the disturbance τ_e is assumed to be an unknown bounded constant. It leads to the following state-space representation:

$$\begin{aligned} \dot{\mathbf{x}} &= \mathbf{f}(\mathbf{x}, \mathbf{u}, \mathbf{w}) \\ \mathbf{y} &= \mathbf{h}(\mathbf{x}) = \mathbf{x}_1 \end{aligned} \tag{8}$$

where $\mathbf{f} := \begin{bmatrix} \mathbf{x}_2 \\ N(\mathbf{x}_1)\left(\boldsymbol{\phi}(\mathbf{x}_1, \mathbf{x}_2) + \mathbf{u} + \mathbf{w}\right) \end{bmatrix}$, $N(\mathbf{x}_1) := \mathcal{M}^{-1}(\mathbf{x}_1)$ and $\boldsymbol{\phi}(\mathbf{x}_1, \mathbf{x}_2) := -\mathcal{C}(\mathbf{x}_1, \mathbf{x}_2)\mathbf{x}_2 - \mathcal{D}\mathbf{x}_2 - \mathcal{K}(\mathbf{x}_1 - \mathbf{x}_{1,0})$.

The system (8) is passive when $\mathbf{w} = \mathbf{0}$. The definition of a passive system is provided as follows.

Definition 1: [16, Definition 10.4] The nonlinear system (8) with zero disturbance, i.e., $\mathbf{w} \equiv \mathbf{0}$ is said to be passive if there exists a continuously differentiable positive semi-definite function V(x) (called the storage function) such that

$$\mathbf{u}^T\mathbf{y} \geq \frac{\partial V}{\partial \mathbf{x}}\mathbf{f}(\mathbf{x}, \mathbf{u}) + \epsilon\mathbf{u}^T\mathbf{u} + \delta\mathbf{y}^T\mathbf{y} + \rho\psi(\mathbf{x}) \tag{9}$$

where ϵ, δ and ρ are non-negative constants and ϕ is semi-definite function of $\mathbf{x}$ such that $\psi(\mathbf{x}(t)) \equiv 0 \Rightarrow \mathbf{x}(t) \equiv 0$ for all solutions of (8) and any $u(t)$ for which the solution exists.

C. Properties of the dynamic system

The following properties of the Inertia and Coriolis matrices are considered as proposed by Nicosia [17], Ortega [15] and Schjølberg [18].

Commutation property For any $\mathbf{q}$, $\mathbf{x}$ and $\mathbf{y}$ in R^n, it has

$$\mathcal{C}(\mathbf{q}, \mathbf{x})\mathbf{y} = \mathcal{C}(\mathbf{q}, \mathbf{y})\mathbf{x} \tag{10}$$

Principle of conservation of energy For any $\mathbf{q} \in R^n$, the following inequality holds

$$(\dot{\mathbf{q}})^T(\dot{\mathcal{M}} - 2\mathcal{C})\dot{\mathbf{q}} = 0 \tag{11}$$

Limit of the Norm of the Coriolis Matrix There exists $\alpha_c > 0$ such that

$$\left\|C(\mathbf{q}, \dot{\mathbf{q}})\right\| \leq \alpha_c \left\|\dot{\mathbf{q}}\right\|, \alpha_c > 0, \qquad \text{for any} \mathbf{q} \in R^n. \tag{12}$$

The Euler-Lagrange model intuitively relates to the Passivity property of systems, which can be quite useful when designing controllers for mechanical systems. This analysis has been done extensively by Khalil [16], Ortega [15], and Brogliato [19]. Choosing a storage function candidate V as:

$$V = \frac{1}{2}\mathbf{x}_2^T\mathcal{M}(\mathbf{x}_1)\mathbf{x}_2 + \frac{1}{2}(\mathbf{x}_1 - \mathbf{x}_{1,0})^T\mathcal{K}(\mathbf{x}_1 - \mathbf{x}_{1,0}) \tag{13}$$

where $\mathcal{M}$ is the finger inertia matrix and $\mathcal{K}$ is the joint stiffness matrix. Obviously, this storage function is positive definite. Then the derivative of the storage function along

the trajectories of (8) without disturbances can be shown to satisfy the following inequality:

$$\dot{V} \leq -\dot{\mathbf{x}}_1^T \mathcal{D} \dot{\mathbf{x}}_1, \tag{14}$$

where $\mathcal{D}$ is the dissipation matrix. Thus it can be concluded that $\dot{V}$ is negative definite and therefore the system is passive. Thus the state $\mathbf{x}$ is always bounded. It is assumed that

$$\max_{t\geq 0} |\mathbf{q}(t)| \leq \Delta_{x_1}, \quad \max_{t\geq 0} |\dot{\mathbf{q}}(t)| \leq \Delta_{x_2}. \tag{15}$$

D. Control objective

The desired task is the grasp and manipulation of an unknown object using the under-actuated hand. The grasp and manipulation task can be decomposed into the following objectives:

1) Grasp Approach.
2) Grasp Stabilization.
3) Manipulation.

In order to achieve the desired control objective, the framework of System of Funnels developed in [9] will be explored to design a hybrid controller that can control the flow (or switching) among the same system with different control objectives. However, in order to ensure the stability of the overall hybrid system, the first step is to ensure that each subsystem is stable. Most importantly, we need to design the controller for each control objective to guarantee the desired domain attraction as a first step toward to applying the framework of System of Funnels. This paper will focus on the preliminary work that deals with how to ensure the local stability, in terms of Lyapunov, with the desired domain of attraction for Grasp Approach and Grasp Stabilization by applying a simple nonlinear observer based nonlinear PID controller with appropriate controller gain matrices and observer gains. As the contact force control is handled in a similar way as the grasp approach, only the detailed analysis of grasp approach will be provided.

III. Main Results

A. Grasp Approach

Nonlinear PID controller: Usually, the task of grasp can be treated as a position trajectory tracking problem [14]. In order to limit the initial contact to the object (or the collision) so that the trajectory of the system will be bounded when switching to the force controller, a reasonable finger movement is needed. This is usually provided by a good desired trajectory. As tracking is a common control performance requirement, there are many different type control algorithms to achieve the desired tracking performance [14], [15], [5], [4], [3]. Among them, one of the most common used methods is the passivity based control design that can fully explore the passivity of mechanic systems [15], [19].

If the state information $\mathbf{q}$ can be measured, Ortega et. al. [15] proposed a passivity based PID controller for robotic manipulators to track the desired joint angle $\mathbf{q}_{req}$. The advantages of this controller are its simplicity in implementation and robustness. With the limited computational resources a prosthetic device has, this type of controller is quite suitable.

Different from [15], the proposed controller is modified to include an elasticity compensation term to feed forward the control effort required because of the joint springs. It's equivalent to gravity compensation term (the conservative forces) and it can be estimated through a model or experimentally.

The proposed trajectory tracking controller is given by:

$$\boldsymbol{\tau}_1 = \mathcal{K}(\mathbf{x}_1 - \mathbf{x}_{1,0}) - K_{c,p}\tilde{\mathbf{x}}_1 - K_{c,d}\mathbf{x}_2 + \boldsymbol{\varepsilon}_1 \tag{16}$$

$$\dot{\boldsymbol{\varepsilon}}_1 = -K_{c,i}\tilde{\mathbf{x}}_1, \tag{17}$$

where $\tilde{\mathbf{x}}_1 = \mathbf{x}_1 - \mathbf{x}_{1,ref}$. The tuning gain matrices in this controller are $K_{c,p}$, $K_{c,d}$ and $K_{c,i}$. They satisfy that $K_{c,p} = K_{c,p}^T \geq 0$, $K_{c,d} = K_{c,d}^T \geq 0$, $K_{c,i} = K_{c,i}^T \geq 0$ and are diagonal. This controller has the same form as [15, Equations (3.58)-(3.59)] and will be referred to as the Grasp Approach Controller (GAC). The closed-loop consisting of the plant (7) and the controller (17) in the state-space becomes

$$\begin{aligned}
\dot{\tilde{\mathbf{x}}}_1 &= \mathbf{x}_2 \\
\dot{\mathbf{x}}_2 &= \mathcal{M}^{-1}(\tilde{\mathbf{x}}_1 + \mathbf{x}_{1,ref})\left(-\mathcal{C}(\tilde{\mathbf{x}}_1 + \mathbf{x}_{1,ref}, \mathbf{x}_2)\mathbf{x}_2 - \mathcal{D}\mathbf{x}_2\right) \\
&+\mathcal{M}^{-1}(\tilde{\mathbf{x}}_1 + \mathbf{x}_{1,ref})\left(\boldsymbol{\tau}_c + \boldsymbol{\tau}_e - K_{c,p}\tilde{\mathbf{x}}_1 - K_{c,d}\mathbf{x}_2 + \boldsymbol{\varepsilon}_1\right) \\
\dot{\boldsymbol{\varepsilon}}_1 &= -K_{c,i}\tilde{\mathbf{x}}_1 \\
\mathbf{y} &= \tilde{\mathbf{x}}_1 + \mathbf{x}_{1,ref}.
\end{aligned} \tag{18}$$

It is noted that unknown bounded constant disturbance $\boldsymbol{\tau}_e$ can be handled by the integrator.

Denoting $\mathbf{z}_c = \begin{bmatrix} \tilde{\mathbf{x}}_1 & \mathbf{x}_2 & \boldsymbol{\varepsilon}_1 \end{bmatrix}^T$, then the stability properties of closed-loop system (18) were provided in [15, Proposition 3.18]. It was shown that the PID (18) is only locally output strictly passive and locally uniformly globally asymptotically stable (UGAS). The domain of attraction can be estimated using some Lyapunov functions.

However, the proposed nonlinear PID controller (17) requires the measurements of $\mathbf{x}$ which includes $\dot{\mathbf{q}}$. Usually, it is easy to measure the positions q_p and q_d while it is not easy to measure $\dot{q}_p$ and $\dot{q}_d$. There are many numerical methods that have been used to estimate $\dot{q}_p$ and $\dot{q}_d$ from the position measurements [6]. These numerical methods can work well provided that there are no high frequency noises in the measurements. But the stability analysis of using numerical methods is still lacking.

Next a nonlinear observer is designed to estimate the needed state (joint position and joint velocities) for the nonlinear PID controller (17).

Nonlinear observer based nonlinear PID control: The role of the observer is to estimate the joint velocities. Nicosia [17] proposed a nonlinear observer designed for this purpose. Consequently, the observer takes the following form:

$$\begin{aligned}
\dot{\hat{\mathbf{x}}}_1 &= \hat{\mathbf{x}}_2 + K_{o,d}\tilde{\mathbf{x}}_1 \\
\dot{\hat{\mathbf{x}}}_2 &= \mathcal{M}(\mathbf{y})^{-1}\left(-\mathcal{C}(\mathbf{y}, \hat{\mathbf{x}}_2)\dot{\hat{\mathbf{x}}}_1 - \mathcal{D}(\hat{\mathbf{x}}_2) - \mathcal{K}(\mathbf{y} - \mathbf{x}_{1,0})\right) \\
&\quad +\mathcal{M}(\mathbf{y})^{-1}\left(-K_{o,p}\tilde{\mathbf{x}}_1 + \boldsymbol{\tau}_1 + \boldsymbol{\tau}_c\right)
\end{aligned} \tag{19}$$

where $\boldsymbol{\tau}_1$ comes from (16), $\boldsymbol{\tau}_c$ is measurable, and matrices $K_{o,p}$ and $K_{o,d}$ are design parameters. They are selected such that $K_{o,p} = K_{o,p}^T \geq 0$ and $K_{o,d} = K_{o,d}^T \geq 0$ are diagonal.

The closed-loop system that consists the observer (19), the controller $\hat{\boldsymbol{\tau}}_1$ (using $\hat{\mathbf{x}}_2$ instead of $\mathbf{x}_2$ in (16)) and the plant

has the following form:

$$\begin{aligned}
&\dot{\tilde{\mathbf{x}}}_1 = \mathbf{x}_2 \\
&\dot{\mathbf{x}}_2 = \mathcal{M}^{-1}(\tilde{\mathbf{x}}_1 + \mathbf{x}_{1,ref})\left(-\mathcal{C}(\tilde{\mathbf{x}}_1 + \mathbf{x}_{1,ref}, \mathbf{x}_2)\mathbf{x}_2 - \mathcal{D}\mathbf{x}_2\right) \\
&+\mathcal{M}^{-1}(\tilde{\mathbf{x}}_1 + \mathbf{x}_{1,ref})\left(\boldsymbol{\tau}_c + \boldsymbol{\tau}_e - K_{c,p}\tilde{\mathbf{x}}_1 - K_{c,d}\hat{\mathbf{x}}_2 + \boldsymbol{\varepsilon}_1\right) \\
&\dot{\boldsymbol{\varepsilon}}_1 = -K_{c,i}\tilde{\mathbf{x}}_1 \\
&\dot{\tilde{\mathbf{x}}}_1 = \hat{\mathbf{x}}_2 + K_{o,d}\tilde{\mathbf{x}}_1 \\
&\dot{\hat{\mathbf{x}}}_2 = \mathcal{M}(\mathbf{y})^{-1}\left(-\mathcal{C}(\mathbf{y}, \hat{\mathbf{x}}_2)\dot{\hat{\mathbf{x}}}_1 - \mathcal{D}(\hat{\mathbf{x}}_2) - \mathcal{K}(\mathbf{y} - \mathbf{x}_{1,0})\right) \\
&+\mathcal{M}(\mathbf{y})^{-1}\left(-K_{o,p}\tilde{\mathbf{x}}_1 + \boldsymbol{\tau}_1 + \boldsymbol{\tau}_c\right) \qquad (20)
\end{aligned}$$

Denoting $\mathbf{z} := \begin{bmatrix} \tilde{\mathbf{x}}_1 & \mathbf{x}_2 & \mathbf{z}_1 & \mathbf{z}_2 & \boldsymbol{\varepsilon}_1 \end{bmatrix}^T$ where $\mathbf{z}_1 = \hat{\mathbf{x}}_1 - \mathbf{x}_1$ and $\mathbf{z}_2 = \hat{\mathbf{x}}_2 - \mathbf{x}_2$ and $M_{max} = \max_{\mathbf{q}\in\Delta_{x_1}} \lambda_{max}(\mathcal{M}(q))$, and $M_{min} = \max_{\mathbf{q}\in\Delta_{x_1}} \lambda_{min}(\mathcal{M}(q))$ where Δ_{x_1} comes from (15), the first main result is presented as follows. Due to the space limitation, only a sketched proof is provided.

Theorem 1: For any given $\Delta_{x_1} > 0$, $\Delta > \Delta_{x_1}$, $\mathcal{D} = \mathcal{D}^T > 0$ and any constant $\boldsymbol{\tau}_e$, there exists $K_{c,d}^T(\Delta_{x_1}, \mathcal{D}, \boldsymbol{\tau}_e) = K_{c,d}(\Delta_{x_1}, \mathcal{D}, \boldsymbol{\tau}_e) > 0$ such that

$$\lambda_{min}(K_{c,d}) > M_{max} - \lambda_{min}(\mathcal{D}) + \alpha_c\Delta_{x_1}, \qquad (21)$$

such that any $K_{c,i} = K_{c,i}^T > 0$ and the selected $K_{c,d}$, there exists $K_{c,p}(K_{c,i}, K_{c,d}, \Delta_{x_1}, \mathcal{D}, \boldsymbol{\tau}_e) = K_{c,p}^T(K_{c,i}, K_{c,d}, \Delta_{x_1}, \mathcal{D}, \boldsymbol{\tau}_e) > 0$ such that

$$\lambda_{min}(K_{c,p}) > \max\{\lambda_{max}(K_{c,i}), \delta_1\} \qquad (22)$$

where

$$\delta_1 := M_{max} - \lambda_{min}(\mathcal{D}) + \lambda_{max}(K_{c,i}) - \lambda_{min}(K_{c,d}), \qquad (23)$$

such that there exists a positive constant $K_{o,d} = K_{o,d}(\Delta, K_{c,i}, K_{c,d}, K_{c,p}\Delta_{x_1}, \mathcal{D}, \boldsymbol{\tau}_e)$ such that there exists a class $\mathcal{KL}$ function β such that the trajectories of the system (20) satisfy

$$|\mathbf{z}(t)| \leq \beta(|\mathbf{z}(0)|, t) \qquad (24)$$

for all $|\mathbf{z}(0)| \leq \Delta$. ∘

Sketch of proof: The the following Lyapunov candidate $V(\mathbf{z}) = \mathbf{z}^T\mathcal{B}(\mathbf{y})\mathbf{z}$ is selected in which

$$\mathcal{B}(\mathbf{y}) := \begin{bmatrix} K_{c,p} + \mathcal{D} + K_{c,d} & \mathcal{M}(\mathbf{y}) & 0 & 0 & -1 \\ \mathcal{M}(\mathbf{y}) & \mathcal{M}(\mathbf{y}) & 0 & 0 & 0 \\ 0 & 0 & K_{o,p} & 0 & 0 \\ 0 & 0 & 0 & \mathcal{M}(\mathbf{y}) & 0 \\ -1 & 0 & 0 & 0 & \frac{1}{K_{c,i}} \end{bmatrix}$$

is positive definite.

The derivative of this Lyapunov function along the trajectories of (20) satisfies:

$$\dot{V}(\mathbf{z}) \leq -\begin{bmatrix} \tilde{\mathbf{x}}_1 \\ \mathbf{x}_2 \\ \mathbf{z}_2 \end{bmatrix}^T \begin{bmatrix} \Lambda_1 & 0 & \Psi_1 \\ 0 & \Phi_1 & \Psi_1 \\ \Psi_1 & \Psi_1 & \Omega_1 \end{bmatrix} \begin{bmatrix} \tilde{\mathbf{x}}_1 \\ \mathbf{x}_2 \\ \mathbf{z}_2 \end{bmatrix} \qquad (25)$$

where:

$$\begin{aligned}
\Lambda_1 &= \lambda_{min}(K_{c,p}) - \lambda_{max}(K_{c,i}) \\
\Psi_1 &= -\frac{\lambda_{max}(K_{c,d})}{2} \\
\Phi_1 &= \lambda_{min}(\mathcal{D}) + \lambda_{min}(K_{c,d} - M_{max} - \alpha_c\Delta_{x_1} \\
\Omega_1 &= K_{o,d}M_{min} + \lambda_{min}(\mathcal{D}) - \alpha_c\left[\left\|\mathbf{x}_2\right\| + \left\|\mathbf{z}_2\right\|\right]
\end{aligned}$$

By using the tuning matrices of nonlinear PID controller and parameter $K_{o,d}$ of the observer, the derivative of this Lyapunov function along the trajectories of (20) is negative semi-definite. By applying Krasovskii-LaSalle's invariance principle similar to [15, Chapter 3], the proof is completed. □

Remark 1: It is important to note that, as expected, the stability of the closed loop feedback system will be determined by the controller gains and the observer gain $K_{o,d}$. Theorem 1 provides the tuning sequences for PID gains and observer gains. The observer gain $K_{o,d}$ plays an important role in order to achieve the given domain of attraction so that it is large enough $\Delta > \Delta_{x_1}$ for selected controller gain matrices. This agrees with Khalil's high gain observer conditions for stability [20]. ∘

Remark 2: Even though stability properties of PID controller [15] and nonlinear observer [17] have been shown independently, to the best of authors' knowledge, there is no proof to show that the nonlinear observer based PID controller is also stable. As the closed-loop system is nonlinear, the Separation Principle does not hold. Although, the high gain observer design method [20] is not directly applied in the stability analysis, the stability result using the Lyapunov function also indicates that the observer gain needs to be high enough to achieve the desired domain attraction. ∘

Remark 3: There is a clear performance trade-off between the domain of attraction and control efforts. If a larger Δ is needed, a higher gain observer is needed. This leads to possible large control input signal in the transient response. In future, experiments will be conducted to find out the best balance between the domain of attraction and control effort that are coming from hardware setting. ∘

B. Grasp stabilization and Contact force stability

Grasp stabilization: The grasp stabilization follows the similar design procedure. It uses a standard PID control structure as the GAC assuming that $\dot{\mathbf{q}}$ is measurable:

$$\begin{aligned}
\mathbf{u}_2 = \boldsymbol{\tau}_2 &= \mathcal{K}(q - q_0) - K_{d,p}\tilde{\mathbf{F}}_c - K_{f,d}\dot{\mathbf{q}} + \varepsilon_2 \\
\dot{\varepsilon_2} &= -K_{f,i}\tilde{\mathbf{F}}_c \qquad (26)
\end{aligned}$$

where $\tilde{F}_c = F_c - F_{c,ref}$ with the desired constant contact force $F_{c,ref}$. Here $K_{f,p}$, $H_{f,d}$ and $K_{f,i}$ are symmetric positive definite gain matrices to ensure the stability of the closed-loop. When $\dot{\mathbf{q}}$ is not measurable, the same observer is used with a different set of tuning matrices and gains that can locally stabilize the grasp procedure. Similar to nonlinear observer used for the GAC, the gain of nonlinear observer has been selected sufficiently large in order to achieve the desired domain of attraction.

Contact force stability: In [6] and [21] is established that it is possible to represent the force tracking objective $\mathbf{F}_{c,ref}$ as a position tracking objective $\mathbf{q}_{ref}$. Given that the finger is in contact with an object, the contact force $\mathbf{F}_c$ can be mapped to a virtual position state $\mathbf{q}_v$ such that:

$$\mathbf{q}_v(t) = \mu(\mathbf{F}_c(t)), \forall\mathbf{F}_c(t) > 0 \qquad (27)$$

where $\mu(\mathbf{F}_c(t))$ is a mapping function that satisfies the contact relationship such that $\mathbf{q}_v \rightarrow \mathbf{q}_{ref}$ implies $\mathbf{F}_c \rightarrow \mathbf{F}_{c,ref}$. When the mapping is known, it is possible to convert the force tracking error $\tilde{\mathbf{F}}_c$ to the virtual state tracking in

terms of $\tilde{\mathbf{q}}_v$. Therefore $\tilde{\mathbf{q}}_v \to 0$ implies $\tilde{\mathbf{F}}_c \to 0$ [6]. Under such a situation, the stability analysis of the CFC controller can be performed in a similar fashion as the GAC controller.

IV. Simulations

The under-actuated finger model was simulated using MATLAB/Simulink. Only nonlinear observer based GAC is simulated, though simulations of nonlinear observer based CFC showed the similar performance. Table II shows the model parameters, observer parameters, the GAC parameters used in the simulation.

Property	Description	Property	Description
l_p, l_d	0.1 (m)	r_d	0.012 (m)
r_p	0.02 (m)	m_d	0.02 (kg)
m_p	0.02 (kg)	k_d	0.185 (N-m/rad)
k_p	0.043 (N-m/rad)	q_{d0}	π/3 (rad)
q_{p0}	π/10 (rad)	$K_{o,d}$	500
$K_{o,p}$	5.8	$K_{c,d}$	0.03
$K_{c,p}$	5.8	$K_{c,i}$	1

TABLE II
Simulation parameters.

The performance of proposed nonlinear observer based GAC ($GAC + Observer$) is compared with the GAC using numerical differentiator method ($GAC + NumDiff$) method with the consideration of high frequency measurement noise disturbances. This disturbance was given by a sinusoidal wave with a frequency of 5000 rad/sec. Figure 2 shows the performance comparison between $GAC + Observer$ and $GAC + NumDiff$. It can be clearly seen that the Numeric Differentiator suffers from high noise sensitivity and performance degradation, while the observer retains the desirable performance. The similar performance can be observed from nonlinear observer based CFC in terms of robustness with respect to high frequency measurement noises. Other simulations also show that the domain of attraction will be increased by increasing $K_{o,d}$.

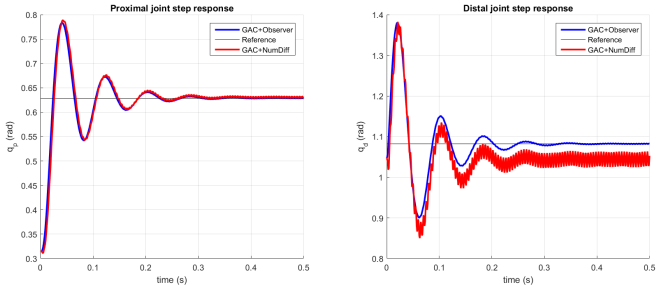

Fig. 2. Tracking performance comparison.

V. Conclusion

This paper presents a nonlinear observer based nonlinear PID controller for a class of under-actuated compliant robotic hand to achieve the Grasp Approach and Grasp Stabilization. By tuning parameters of nonlinear observer and PID controller appropriately, it is possible to achieve the desired local stability with the given domain attraction and constant disturbance rejection. The obtained controllers will serve as basic components in order to design a proper hybrid control under the framework of System of Funnels, which provides stability guarantees for the hybrid controller, to achieve the desired control objectives with the consideration of the switching among different control laws for each subsystem. The presented work lays the foundations required for the development of a System of Funnels hybrid controller for the complex task, which will be addressed in future work.

References

[1] Z. Xu and E. Todorov, "Design of a Highly Biomimetic Anthropomorphic Robotic Hand towards Artificial Limb Regeneration," in *IEEE International Conference on Robotics and Automation*, 2016.

[2] L. Zollo, S. Roccella, E. Guglielmelli, M. C. Carrozza, and P. Dario, "Biomechatronic design and control of an anthropomorphic artificial hand for prosthetic and robotic applications," in *IEEE/ASME Transactions on Mechatronics*, vol. 12, no. 4, 2007, pp. 418–429.

[3] Y. T. Lee, H. R. Choi, W. K. Chung, and Y. Youm, "Stiffness Control of a Coupled Tendon-Driven Robot Hand," *IEEE Control Systems*, vol. 14, no. 5, pp. 10–19, 1994.

[4] H. Luo, X. Duan, and H. Deng, "Sliding Mode Impedance Control of a Underactuated Prosthetic Hand," in *Proceeding of the IEEE International Conference on Information and Automation*, 2014, pp. 726–729.

[5] R. Kubo and K. Ohnishi, "Hybrid Control for Multiple Robots in Grasping and Manipulation," *2006 12th International Power Electronics and Motion Control Conference*, vol. 1, no. 2, pp. 367–372, 2006.

[6] D. Heck, A. Saccon, N. van de Wouw, and H. Nijmeijer, "Switched position-force tracking control of a manipulator interacting with a stiff environment," in *American Control Conference (ACC), 2015*. IEEE, 2015, pp. 4832–4837.

[7] A. Majumdar, A. A. Ahmadi, and R. Tedrake, "Control design along trajectories with sums of squares programming," in *Proceedings - IEEE International Conference on Robotics and Automation*, 2013, pp. 4054–4061.

[8] A. Majumdar and R. Tedrake, "Robust online motion planning with regions of finite time invariance," in *Algorithmic Foundations of Robotics X: Proceedings of the Tenth Workshop on the Algorithmic Foundations of Robotics*. Berlin, Heidelberg: Springer Berlin Heidelberg, 2013, pp. 543–558.

[9] R. Shvartsman, "System of Funnels Framework for Robust Non-linear Control," Ph.D. dissertation, The University of Melbourne, 2015.

[10] R. Balasubramanian, J. T. Belter, and A. M. Dollar, "External disturbances and coupling mechanisms in underactuated hands," *Proceedings of IDETC, Montreal, Quebec*, 2010.

[11] A. M. Dollar and R. D. Howe, "The Highly Adaptive SDM Hand: Design and Performance Evaluation," *The International Journal of Robotics Research*, vol. 29, no. 5, pp. 585–597, 2010.

[12] R. Balasubramanian, J. T. Belter, and A. M. Dollar, "Disturbance Response of Two-Link Underactuated Serial-Link Chains," *Journal of Mechanisms and Robotics*, vol. 4, no. 2, p. 021013, 2012.

[13] L. Birglen, T. Laliberté, and C. M. Gosselin, *Underactuated Robotic Hands*. Springer-Verlag Berlin Heidelberg, 2007, vol. 40.

[14] R. M. Murray, Z. Li, and S. S. Sastry, *A Mathematical Introduction to Robotic Manipulation*. CRC Press, 1994, vol. 29.

[15] R. Ortega, A. Loría, P. J. Nicklasson, and H. Sira-Ramírez, *Passivity-based Control of Euler-Lagrange Systems Mechanical, Electrical and Electromechanical Applications*. Springer-Verlag London Ltd., 1998.

[16] H. K. Khalil and J. Grizzle, *Nonlinear Systems*, 3rd ed. Pearson, 2002.

[17] S. Nicosia and P. Tomei, "Robot control by using only joint position measurements," *IEEE Transactions on Automatic Control*, vol. 35, no. 9, pp. 1058–1061, 1990.

[18] P. J. From, I. Schjølberg, J. T. Gravdahl, K. Y. Pettersen, and T. I. Fossen, "On the boundedness and skew-symmetric properties of the inertia and coriolis matrices for vehicle-manipulator systems," in *Intelligent Autonomous Vehicles*, vol. 7, no. 1, 2010, pp. 193–198.

[19] B. Brogliato, R. Lozano, B. Maschke, and O. Egeland, *Dissipative Systems Analysis and Control*, 2nd ed. Springer-Verlag London Ltd., 2007.

[20] H. K. Khalil and L. Praly, "High-gain observers in nonlinear feedback control," *International Journal of Robust and Nonlinear Control*, vol. 24, no. 6, pp. 993–1015, apr 2013.

[21] H. Zhang, Z. Zhen, Q. Wei, and W. Chang, "The position/force control with self-adjusting select-matrix for robot manipulators," in *Robotics and Automation, 2001. Proceedings 2001 ICRA. IEEE International Conference on*, vol. 4. IEEE, 2001, pp. 3932–3936.